

Tunneling-CNTFETs

M. Pourfath, H. Kosina, and S. Selberherr

Institute for Microelectronics, TU Wien, Gußhausstraße 27–29/E360, 1040 Wien, Austria

e-mail: pourfath@iue.tuwien.ac.at

INTRODUCTION

Exceptional electronic and mechanical properties together with nanoscale diameter make carbon nanotubes (CNTs) candidates for nanoscale field effect transistors (FETs). High performance CNTFETs were achieved recently [1, 2]. Metallic contacts can be directly connected to the gate-controlled CNT channel [1]. To reduce the parasitic capacitances the spacing between the gate-source and the gate-drain contacts can be increased. The extension region can be of n or p-type leading to $n/i/n$ or $p/i/p$ devices. Unlike conventional semiconductors, in which doping is introduced by implantation, doping of CNTs requires controlling the electrostatics of the CNT environment by additional gates [2], molecules [3], or metal ions [4]. The gate controls the thermionic emission current, therefore a sub-threshold slope of about 64 mV/dec can be achieved [2]. Aggressively scaled devices of this type suffer from charge pile-up in the channel [5], which deteriorates the off-current substantially and ultimately limits the achievable I_{on}/I_{off} ratio [5].

In order to overcome this obstacle a gate-controlled tunneling device (T-CNTFET) has been proposed [5]. In this type of device either a $p/i/n$ or $n/i/p$ doping profile can be used. The gate voltage controls the band bending at the junctions, which modulates the band to band tunneling current. The T-CNTFET benefits from a steep inverse sub-threshold slope and a better controlled off-current.

SIMULATION RESULTS

In this work we present a numerical study of a T-CNTFET. Because of strong quantum effects, the non-equilibrium Green's function (NEGF) formalism has been chosen to investigate the behavior of these devices. Ballistic transport is assumed and the coupled transport and Poisson equations have

been solved. We studied the effect of the doping concentration on the device performance.

The operation of the device can be well understood by considering the spectrum of electrons along the device (Fig.3 and Fig.5). At high negative gate voltages, due to strong band bending near the source contact, band to band tunneling contributes greatly to the total current. By increasing the gate voltage to positive values the band bending near the source contact decreases, and as a result band to band tunneling decreases. On the other hand the increase of the gate voltage results in a strong band to band tunneling near the drain contact, see Fig.3 ($V_{GS} = -0.6V$). As a result the total current increases in the off regime which has a detrimental effect on the device performance (Fig.2). In the device we discussed, the doping concentrations at the source and drain sides are assumed to be equal. By decreasing the doping of the drain side the band bending decreases for the same gate voltage (Fig.5) and the band to band tunneling current near the drain contact decreases greatly, see Fig.2 and Fig.4.

CONCLUSION

We performed numerical investigation of a T-CNTFET. Due to strong quantum effects including band to band tunneling, the NEGF formalism along with complex band structure gives a suitable model for the analysis of these devices. Simulation results suggest that an asymmetric doping concentration reduces the parasitic carrier injection and increases the I_{on}/I_{off} ratio by several orders of magnitude.

ACKNOWLEDGMENT

This work has been partly supported by the Austrian Science Fund FWF, project 17285-N02 and the National Program for Tera-level Nano-devices of the Korean Ministry of Science and Technology.

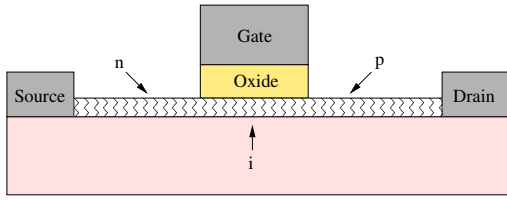


Fig. 1. T-CNTFET device with n/i/p doping profile.

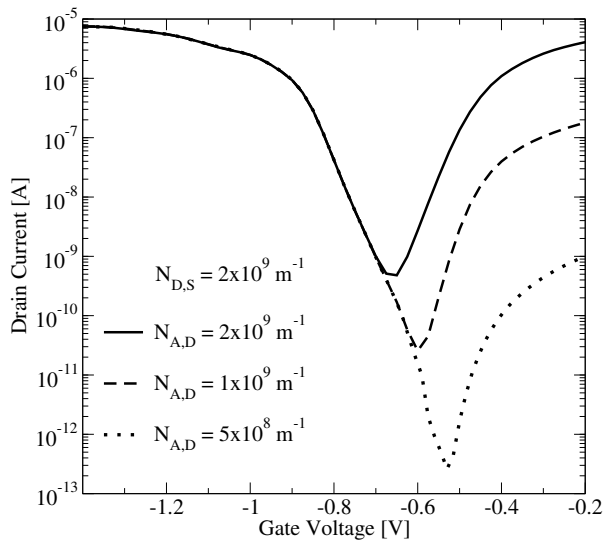


Fig. 2. Transfer characteristics for different doping profiles.

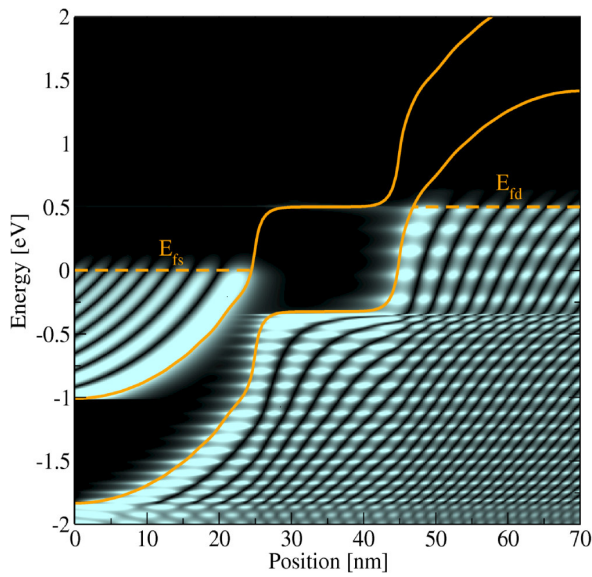


Fig. 3. The distribution of electrons in energy space along the device with $N_{D,S} = 2 \times 10^9 \text{ m}^{-1}$ and $N_{A,D} = 2 \times 10^9 \text{ m}^{-1}$.

REFERENCES

- [1] A. Javey *et al.*, Nano Lett. **4**, 1319 (2004).
- [2] Y.M. Lin *et al.*, IEEE Trans.Nanotechnology **4**, 481 (2005).
- [3] J. Chen *et al.*, in *IEDM Tech.Dig.* 695 (2004)
- [4] A. Javey *et al.*, Nano Lett. **5**, 345 (2005).
- [5] J. Appenzeller *et al.*, **52**, 2568 (2005).
- [6] R. Venugopal *et al.*, J.Appl.Phys. **92**, 3730 (2002).

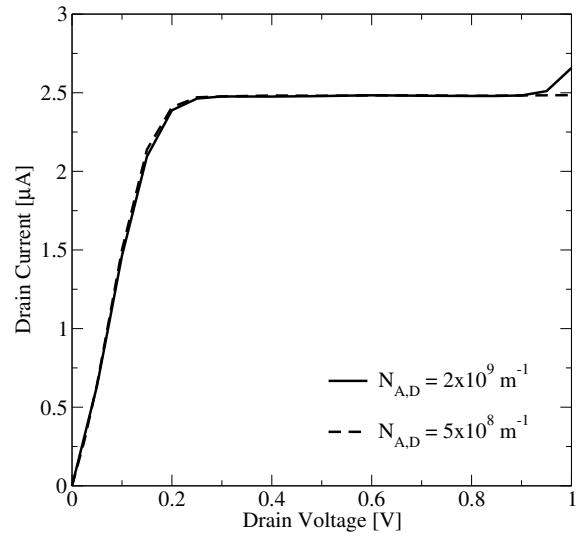


Fig. 4. Output characteristics for different doping profiles.

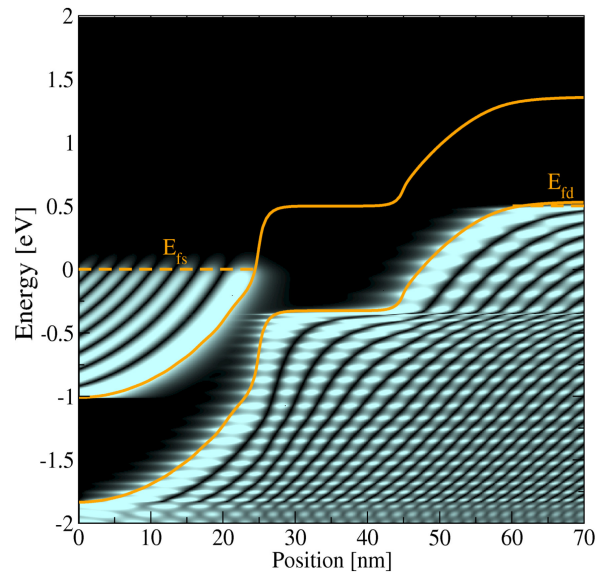


Fig. 5. The distribution of electrons in energy space along the device with $N_{D,S} = 2 \times 10^9 \text{ m}^{-1}$ and $N_{A,D} = 5 \times 10^8 \text{ m}^{-1}$.